

Stepwise Assembly of Nanoparticles, -tubes, -rods, and -wires in Reverse Micelle Systems

Yun Chen,^[a] Qingsheng Wu,^{*[a]} and Yaping Ding^[b]

Keywords: Stepwise-assembly synthesis / Nanomaterials / $\text{CaSO}_4 \cdot 2\text{H}_2\text{O}$ / Reverse micelles

A traditional facile method was used for the stepwise-assembly synthesis of $\text{CaSO}_4 \cdot 2\text{H}_2\text{O}$ nanoparticles, -tubes, -rods, and -wires. Sizes of these nanostructures vary from tens of nanometers to tens of microns. The key point of the stepwise-assembly process is the reaction time. The growth process was studied as a function of the reaction time and this was used to guide the synthesis of other one-dimensional nanomaterials in reverse micelle systems. The results showed that

this growth process is somewhat universal in synthesizing inorganic salts with zero/one-dimensional and solid/hollow structures in reverse micelle systems. The growing mechanism was also explored and it was believed to be an assembly-based growth in association and concurrent with the surfactant-templating mechanism.

(© Wiley-VCH Verlag GmbH & Co. KGaA, 69451 Weinheim, Germany, 2007)

Introduction

The reverse micelle or microemulsion system is a traditional synthesis method that has been widely used to prepare nanomaterials because of its facility, speediness, and efficiency. Being a soft template system with affluent diversification, reverse micelles were used to fabricate nanomaterials with different novel morphologies.^[1–14] However, it is the variety that makes it difficult to effectively control the morphology. Thus, how to regulate the shapes and structures effectively in reverse micelle systems has become the target that most scientists seek. Although considerable efforts have been made to control the synthesis at will in reverse micelle systems,^[15–19] to date no one has achieved the successful synthesis of a series of different nanostructures in one reverse micelle system. Somewhat controllable methods are involved such as changing surfactant concentration, reactant concentration, ω_0 , and using different surfactants.^[20–22] In these methods it is found that the structures of the micelle templates are changed fundamentally to tune nanostructures. However, the structures and behavior of micelle templates are still not clear so much uncertainty is involved in these methods. Consequently there is an urgent need to explore the entire picture of the growth process in such a system.

The development of nanoscience and -technology over the last two decades shows that some interesting new nano-

structures can be fabricated based on the mechanism called “oriented attachment”.^[23–24] In this mechanism, inorganic nanocrystals are the fundamental building blocks for the creation of highly ordered extended nanostructures. Although there are now feasible ways for the formation of low-dimensional complex nanostructures using nanoparticles as building blocks,^[25] the challenge for the organization of nanoparticles into higher dimensional structures still remains. Nanotubes are higher structures constructed by initial nano building blocks and are thought to be a sort of the most promising nanomaterials.^[26–27] However, most of the obtained nanotubes are oxides or have graphite-like structures.^[28–32] noncarbon, nonoxide, and nonlaminated nanotubes are difficult to fabricate through ordinary methods.^[33–34] The simple and easy way to make nanotubes at room temperature described in this paper can offer more opportunities for the research of noncarbon, nonoxide, and nonlaminated nanotubes.

Reaction time was investigated as an impact factor in the microemulsion system and its main role is believed to be to control the crystal growth and crystallinity.^[5,35] However, after many trials other important functions of aging time were discovered. It can control the dimension, morphology, and structure of the products under certain circumstances. In this work, by controlling reaction time step by step, according to the characteristics of different inorganic salts, stepwise-assembly synthesis of non-oxide ionic-crystal nanomaterials from nanoparticles to nanotubes, nanorods, and nanowires is successfully realized for the first time in reverse micelle soft-template systems. Thus this study provides a new route in selectively synthesizing low-dimensional nanomaterials in identical reverse micelle systems. It can also bring new vitality to this traditional facile synthesis method.

[a] Department of Chemistry, Tongji University, Shanghai, P. R. China, 200092
E-mail: qswu@mail.tongji.edu.cn

[b] Department of Chemistry, Shanghai University, Shanghai, P. R. China, 200444

Supporting information for this article is available on the WWW under <http://www.eurjic.org> or from the author.

Results and Discussion

Results

The phase composition and phase structure of the samples were examined by X-ray powder diffraction (XRD). Because samples with different shapes all have the same composition, only the XRD pattern of the nanotubular products was given. The products were deposited on a glass base when characterized by XRD. As shown in Figure 1, all of the peaks can be perfectly indexed to a pure monoclinic phase (space group $C2/c^{(15)}$) of $\text{CaSO}_4 \cdot 2\text{H}_2\text{O}$ with lattice constants (a) 6.286 Å, (b) 15.213 Å, and (c) 5.678 Å (JCPDS card No. 33–0311). No other impurities have been detected in the synthesized products. The broad peak between 10 and 30° (2θ) is caused by the amorphous-phase glass base on which the product deposited.

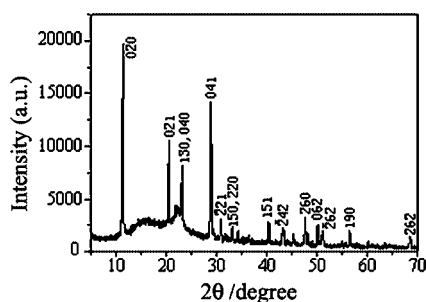


Figure 1. XRD curve of $\text{CaSO}_4 \cdot 2\text{H}_2\text{O}$ obtained in the reverse micelle system.

The morphologies of the synthesized products were examined by transmission electron microscopy (TEM). Figure 2 shows the typical TEM images of the sample prepared in C_{12}E_9 reverse micelles with different reaction times. ω_0 of the reverse micelle was 8 when the concentration of CaCl_2 and Na_2SO_4 was 0.1 M. Tunable shapes of CaSO_4 nanocrystals can be readily produced at different reaction times.

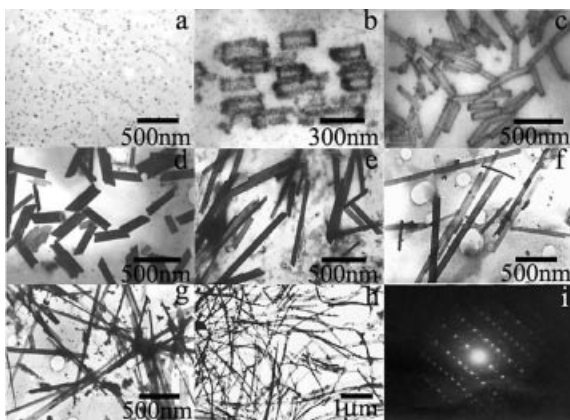


Figure 2. TEM and SAED images of $\text{CaSO}_4 \cdot 2\text{H}_2\text{O}$ at different aging times: (a) 1 min, (b) 3 min, (c) 5 min, (d) 40 min, (e) 3 h, (f) 12 h, (g) 36 h, (h) 108 h, (i) SAED image.

As shown in Figure 2 (a), the products are primarily nanoparticles with a diameter of about 15 nm when the reaction time is 1 min; there are some signals showing nanoparticles tending to form a one-dimensional morphology. This trend is realized when the reaction time extends to 3 min. Nanotubes with a diameter of about 50 nm and a length of nearly 200 nm are formed as shown in part b of Figure 2. From further observations it can be seen that the walls of the nanotubes are composed of nanoparticles, and that the walls become solid when the reaction time is 5 min. But there are few changes in the size of the nanotubes (see Figure 2, c). This process can be described as the assembly from nanoparticles to nanotubes and the increase in the firmness of the nanotubes. The simple method reported in this paper can produce inorganic salt nanotubes at room temperature, which provides a contribution to the research on nanotubes.

Interestingly, when the reaction time is prolonged to 40 min well-dispersed short rods are observed (Figure 2, d), and the growth of the rods keeps for tens of hours as revealed in parts d and g of Figure 2. With the extension of the reaction time both the length and the diameter increased and the increment in length was much larger than that in diameter. When the reaction time is long enough rods grow into wires and the lengths reach nearly 100 μm as shown in part h of Figure 2. The Selected Area Electron Diffraction (SAED) image (Figure 2, i) taken from a single nanotube shown in Figure 2 (c) exhibits single-crystalline diffraction dots that can be indexed to the monoclinic structure of $\text{CaSO}_4 \cdot 2\text{H}_2\text{O}$, which is in good agreement with the XRD result presented above.

The experimental results above demonstrate the possibility of synthesizing nanoparticles, nanotubes, nanorods, and nanowires under certain circumstances in reverse micelle systems. Furthermore, it is found that the reaction time has a significant effect on the morphologies and dimensions of the final products. The effect of the reaction time on the shape and size of the nanomaterials is shown in Figure 3. The size becomes larger with an increase in the reaction time, and the curve reveals that the increase in length is much bigger than that in diameter. Thus the aspect ratio is enhanced when the reaction time becomes longer. The size can vary from tens of nanometers to tens of microns.

By tracking the observed results, the growth process shows that nanoparticles assemble to nanotubes, nanorods, and then to nanowires in a step-by-step fashion as the reaction time increases. The aspect ratio increases along with the reaction time. In order to justify this deduction another two inorganic salts have been synthesized by the same method. The results are shown in Figure 4 and Figure 5. Firstly, $\text{Pb}(\text{OH})\text{Cl}$ was prepared in the same reverse micelle system (C_{12}E_9 , *n*-pentanol, cyclohexane and Pb^{2+} , Cl^- water solution) as CaSO_4 . TEM pictures taken at different reaction times are shown in Figure 4. The results demonstrate that the deduced growth process is reasonable. Another experiment was carried out in a different reverse micelle system to justify the growth process. In this system, C_{12}E_9 was replaced by Triton X-100 and CdS nanoparticles, -tubes,

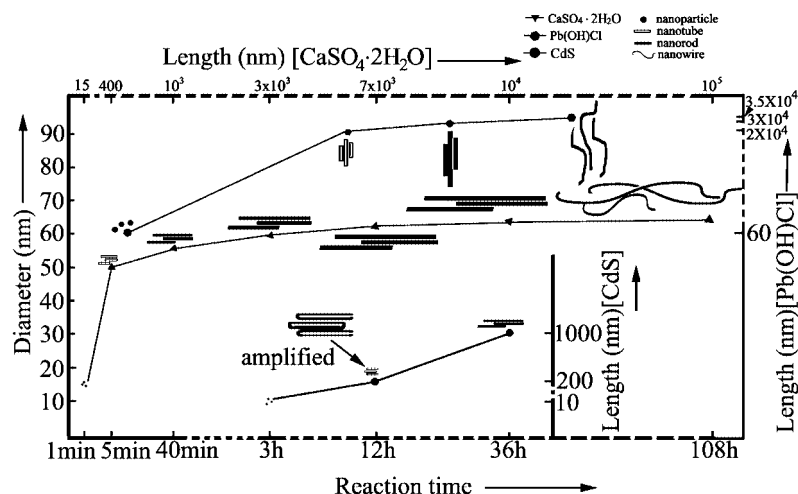


Figure 3. The effect of reaction time on the shape and size of nanomaterials obtained in the reverse micelle systems.

and -rods were prepared stepwise with reaction times becoming longer (as shown in Figure 5). It indicates that the deduction could be used to guide the stepwise-assembly formation in different reverse micelle systems.

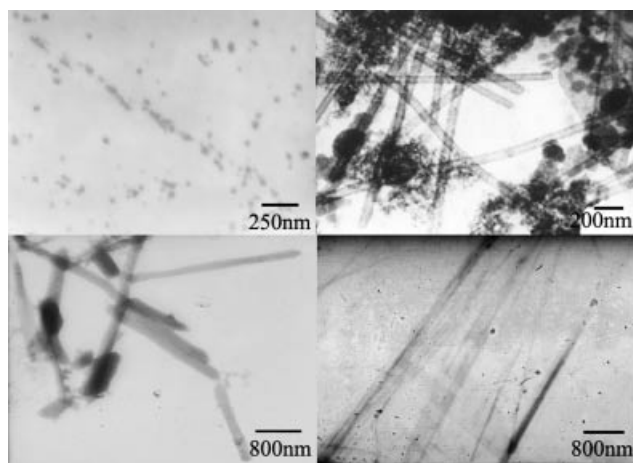


Figure 4. TEM images of as-obtained Pb(OH)Cl nanomaterials in the reverse micelles ($C_{12}E_9$ as surfactant) at different reaction times.

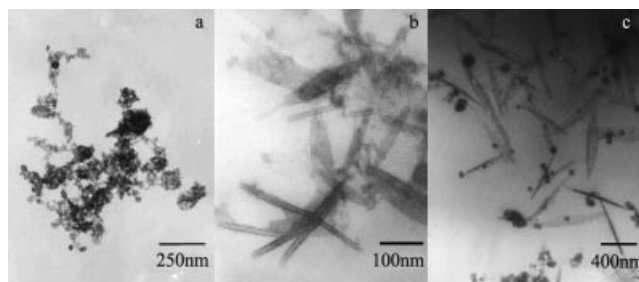


Figure 5. TEM images of CdS obtained in the reverse micelle systems (Triton X-100 as surfactant) at different reaction times: (a) 3 h, (b) 12 h, (c) 36 h.

Similar to the synthesis of CdS, ZnS, and Ag_2S nanoparticles, nanotubes, and nanorods are also synthesized using sulfocarbamide as the sulfur source in the reverse micelle

system (see Supporting Information). All results obtained above show that the stepwise-assembly synthesis has universality in preparing inorganic salts in reverse micelle systems. What is important is that ZnS and Ag_2S nanotubes and nanorods synthesized by this method have never been reported before.

Discussion

The mechanism of stepwise-assembly synthesis is discussed according to the results. The surfactant used in this system is AEO ($C_{12}E_9$), which is a long-chain molecule. It contains two indented hydrophobic and hydrophilic chains, which can easily form a one-dimensional template.^[36] The products obtained in such reverse micelles are commonly one-dimensional materials. The mechanism diagram of the growth procedure is shown in Figure 6.

When two reverse micelle solutions are mixed only micelles containing two different reactants have effective collisions. These effectively collided reverse micelles then fuse and inorganic ions filter to form nucleation. These nuclei grow up to form nanoparticles with micelles attached to the surface. The nanotubes are then assembled in association and concurrent with the self-organization of stacked micellar aggregates (see Figure 7, Figure 2, a and b). It is clearly seen that incompact particles are assembling into wandering tubes, which indicates that nanoparticles are firstly formed and then assembled into tubes. Because these nanotubes are surfactant coated, micelles containing different ions can be absorbed onto the faces by the interaction between the hydrophobic tails of AEO.^[37] When the micelles attach to the surface the surface tension is broken and the ions enter the nanotubes through the interstices of nanoparticles in the wall of the nanotube. Thus different ions react to form $CaSO_4$ nuclei inside nanotubes. These nuclei then grow bigger and the hollow tubes are filled. Lateral growth can still take place since the surfactant- $CaSO_4$ particles are not depleted.^[38] The fact that the size of the nanotubes becomes larger in both length and width is evidence

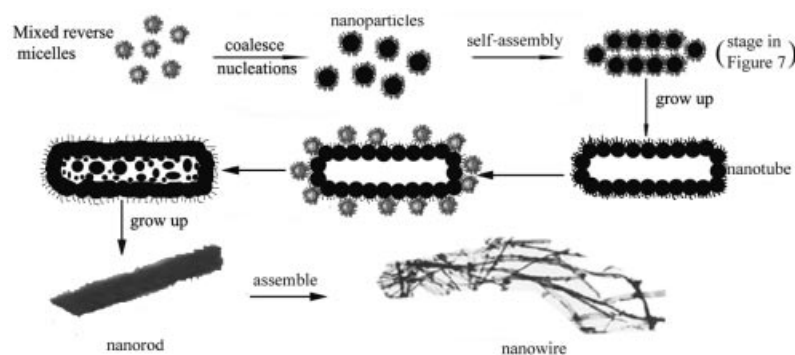


Figure 6. Formation mechanism diagram of stepwise-assembly synthesis.

for this process (Figure 2, b and c). After enough growth nanorods are obtained (Figure 2, d). These short rods coated with surfactant can also assemble into long nanowires with an extension of the aging time (Figure 2, e and f). Thus stepwise-assembly synthesis of nanoparticles, nanotubes, nanorods, and nanowires is successfully realized.

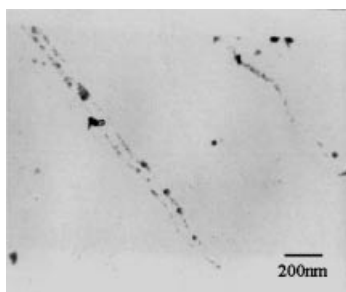


Figure 7. TEM image of Pb(OH)Cl, reaction time is 1 h at 37 °C.

Conclusions

In conclusion, a facile reverse micelle method for the stepwise preparation of CaSO₄ nanoparticles, -tubes, -rods, and -wires in one reverse micelle system is described. By controlling the reaction time in a certain reverse micelle system, CaSO₄ nanocrystals with tunable shapes and sizes are presented. The growth process in this system is deduced to be a stepwise-assembly-growth process. This deduction is demonstrated by several experimental results. This deduction can perceptibly make a contribution not only to the research on inorganic salt nanotubes, nanorods, and nanowires, but also to the application of reverse micelles or microemulsions in fabricating one-dimensional nanomaterials. The products obtained in this work also have potential applications in many fields, such as nanoreactors and drug carriers.

Experimental Section

Reagents: Anhydrous calcium chloride, sodium sulfate, *n*-pentanol, and cyclohexane used in this work were A.R. reagents purchased from Shanghai Chemical Reagent Factory, China. They were used

without any pretreatment. C₁₂E₉ (AEO) [polyoxyethylene (9) dodecyl ether] was used as received from Henkel.

Stepwise Synthesis of CaSO₄ Nanoparticles, Nanotubes, Nanorods, and Nanowires: In a typical procedure a calculated amount of 0.1 M CaCl₂ solution was first placed in a conical flask, and then certain amounts of C₁₂E₉, *n*-pentanol, and cyclohexane were added in turn to form a reverse micelle when stirred vigorously. Another reverse micelle system was prepared through the same method except that the CaCl₂ solution was replaced by a 0.1 M Na₂SO₄ solution. The corresponding volume ratio of Ca²⁺/SO₄²⁻/AEO is 1:1:0.3. Thereafter, the above two reverse micelle solutions were mixed quickly. The mixture was stirred for a few minutes, and then a slightly viscous and optically transparent single-phase liquid was formed. This liquid was then aged for 1 min, 3 min, 5 min, 40 min, 3 h, 12 h, 36 h, and 108 h statically at 30 °C. The solid products were separated by centrifugation and repeatedly washed with anhydrous ethanol. These products were then kept in anhydrous ethanol for further characterization.

Characterization of CaSO₄ Nanomaterials with Different Morphologies: X-ray powder diffraction (XRD) analyses of the products were carried out with a Rigaku D/mx2550 X-ray diffractometer with Cu-K_α radiation ($\lambda = 1.5418 \text{ \AA}$). Transmission electron microscopic (TEM) images were recorded using a Hitachi-800 transmission electron microscope. And the TEM images were obtained on thin films deposited on Cu gauze from a dilute ethanol solution of as-prepared products.

Supporting Information (see also the footnote on the first page of this article): Stepwise synthesis of ZnS and Ag₂S nanoparticles, nanotubes and nanorods. Two figures with transmission electron microscopy images (ZnS at different reaction times and Ag₂S after different aging times).

Acknowledgments

The authors are grateful for the financial support from the National Natural Science Foundation of China (grant numbers 20471042, 20571051), the State Key Project of Fundamental Research (973 Project) for Nanoscience and Nanotechnology (grant number 2006CB932300) and the Nano-Foundation of Shanghai in China (grants 0652nm007, 0552nm048).

- [1] S. Mann, G. Ozin, *Nature* **1996**, 382, 313–318.
- [2] X. J. Zhao, R. P. Bagwe, W. H. Tan, *Adv. Mater.* **2004**, 16, 173–176.
- [3] S. P. Moulik, G. C. De, A. K. Panda, B. B. Bhowmik, A. R. Das, *Langmuir* **1999**, 15, 8361–8367.

- [4] D. Ma, M. Li, A. J. Patil, S. Mann, *Adv. Mater.* **2004**, *16*, 1838–1841.
- [5] Z. L. Yin, Y. Sakamoto, J. H. Yu, S. X. Sun, O. Terasaki, R. R. Xu, *J. Am. Chem. Soc.* **2004**, *126*, 8882–8883.
- [6] B. Yoon, C. M. Wai, *J. Am. Chem. Soc.* **2005**, *127*, 17174–17175.
- [7] J. Zhang, X. Ju, Z. Y. Wu, T. D. Hu, Y. N. Xie, Z. J. Zhang, *Chem. Mater.* **2001**, *13*, 4192–4197.
- [8] H. Ohde, F. Hunt, C. M. Wai, *Chem. Mater.* **2001**, *13*, 4130–4135.
- [9] J. H. Xiang, S. H. Yu, X. Geng, B. H. Liu, Y. Xu, *Cryst. Growth Des.* **2005**, *5*, 1157–1161.
- [10] J. C. Liu, P. Raveendran, Z. Shervani, Y. Ikushima, Y. Hakuta, *Chem. Eur. J.* **2005**, *11*, 1854–1860.
- [11] F. Teng, J. G. Xu, Z. J. Tian, J. W. Wang, Y. P. Xu, Z. S. Xu, G. X. Xiong, *Chem. Commun.* **2004**, 1858–1859.
- [12] T. Tago, T. Hatsuta, K. Miyajima, M. Kishida, S. Tashiro, K. Wakabayashi, *J. Am. Ceram. Soc.* **2002**, *85*, 2188–2194.
- [13] A. J. Zarur, J. Y. Ying, *Nature* **2000**, *403*, 65–67.
- [14] J. P. Ge, S. Xu, L. P. Liu, Y. D. Li, *Chem. Eur. J.* **2006**, *12*, 3672–3677.
- [15] M. M. Wu, J. B. Long, A. H. Huang, Y. J. Luo, S. H. Feng, R. R. Xu, *Langmuir* **1999**, *15*, 8822–8825.
- [16] P. Zhang, L. Gao, *Langmuir* **2003**, *19*, 208–210.
- [17] M. Roth, R. Hempelmann, *Chem. Mater.* **1998**, *10*, 78–82.
- [18] G. B. Sun, M. H. Cao, Y. H. Wang, C. W. Hu, L. Ren, K. L. Huang, *Chem. Commun.* **2005**, 1740–1742.
- [19] M. Haeger, K. Holmberg, *Chem. Eur. J.* **2004**, *10*, 5460–5466.
- [20] M. H. Cao, X. L. Wu, X. Y. He, C. W. Hu, *Langmuir* **2005**, *21*, 6093–6096.
- [21] A. J. Zarur, H. H. Hwu, J. Y. Ying, *Langmuir* **2000**, *16*, 3042–3049.
- [22] G. D. Rees, R. Evans-Gowing, S. J. Hammond, B. H. Robinson, *Langmuir* **1999**, *15*, 1993–2002.
- [23] A. P. Alivisatos, *Science* **2000**, *289*, 736–737.
- [24] R. L. Penn, J. F. Banfield, *Geochim. Cosmochim. Acta* **1999**, *63*, 1549–1557.
- [25] S. A. Davis, M. Breulmann, K. H. Rhodes, B. Zhang, S. Mann, *Chem. Mater.* **2001**, *13*, 3218–3226.
- [26] M. Terrones, W. K. Hsu, H. W. Kroto, D. R. M. Walton, *Top. Curr. Chem.* **1999**, *199*, 189–234.
- [27] M. Remskar, *Adv. Mater.* **2004**, *16*, 1497–1504.
- [28] X. L. Li, Y. D. Li, *Chem. Eur. J.* **2003**, *9*, 2726–2731.
- [29] R. Tenne, *Adv. Mater.* **1995**, *7*, 965–972.
- [30] L. M. Dai, A. Patil, X. Y. Gong, Z. X. Guo, L. Q. Liu, Y. Liu, D. B. Zhu, *ChemPhysChem* **2003**, *4*, 1150–1169.
- [31] C. S. Rout, S. Hari Krishna, S. R. C. Vivekchand, A. Govindaraj, C. N. R. Rao, *Chem. Phys. Lett.* **2006**, *418*, 586–590.
- [32] G. R. Patzke, F. Krumeich, R. Nesper, *Angew. Chem. Int. Ed.* **2002**, *41*, 2446–2461.
- [33] V. V. Pokropivny, *Powder Metall. Met. Ceram.* **2001**, *40*, 485–496.
- [34] H. J. Niu, M. Y. Gao, *Angew. Chem. Int. Ed.* **2006**, *45*, 6462–6466.
- [35] W. Liu, W. Zhong, X. L. Wu, N. J. Tang, Y. W. Du, *J. Cryst. Growth* **2005**, *284*, 446–452.
- [36] X. H. Yang, Q. S. Wu, L. Li, Y. P. Ding, G. X. Zhang, *Colloids. Surf. A* **2005**, *264*, 172–178.
- [37] M. Li, H. Schnablegger, S. Mann, *Nature* **1999**, *402*, 393–395.
- [38] M. Li, S. Mann, *Langmuir* **2000**, *16*, 7088–7094.

Received: February 11, 2007

Published Online: September 12, 2007